

# Evaluation of Indoor Mobile Robot Localization Techniques

<sup>1</sup>Fadi N. Sibai, <sup>2</sup>Hassane Trigui, <sup>3</sup>Pablo Carrasco Zanini, <sup>4</sup>Anwar R. Al-Odail

<sup>1, 2, 3</sup>Saudi Aramco, Research & Development Center, Dhahran 31311, Kingdom of Saudi Arabia

<sup>4</sup>Electrical Engineering Department, King Fahd University for Petroleum and Minerals, Dhahran 31312, Kingdom of Saudi Arabia

Email: {<sup>1</sup>fadi.sibai, <sup>2</sup>hassane.trigui, <sup>3</sup>pablo.carrasco} @aramco.com, <sup>4</sup>anwar\_ab@hotmail.com

## ABSTRACT

Mobile robot localization is an important operation used in several applications. For instance, the location of the mobile robot can be used to associate environment data captured by the robot with the location where this data is captured, or to issue robot commands dependent on location and remaining battery energy. We explore 3 localization methods for indoor robots: optical wheel encoder, ultrasonic sensors, and received WiFi signal strength. We experiment with these localization methods on a National Instruments wheeled DANI robot, compare their accuracies, and evaluate their merits.

**Keywords:** Robot localization; Optical Wheel Encoder; Ultrasonic sensor; WLAN localization.

## 1. INTRODUCTION

Indoor localization is a crucial topic in different engineering fields. It provides the system with the location of people and objects relative to the environment. Recently, indoor localization has been a hot area for several researchers as it solves major issues in our life. These issues may be as simple as protecting a laptop computer from theft or as complicated as a robot recognizing its dynamically changing environment, e.g. NASA's Mars Exploration Rover. Indoor robot localization is considered essential to a mobile robot to reach autonomy. With this critical information, the mobile robot can interact coherently with the environment objects and people and can navigate through the surrounding objects with flexibility in dealing with unexpected situations. Some of these applications are exploring, search and rescue, surveillance, retrieving, transporting, and other missions. The location of the robot may be used in determining the robot's next action or in issuing the proper command to the robot or in logging sensor data with the corresponding location where the sensor data was retrieved. For all these reasons, it is important that the task of localization be performed accurately, since the acquisition of inaccurate localization data causes an imperfect implementation of the operation. Thereafter, it is important to identify a reliable localization method for indoor mobile robots.

In this paper, we will describe and compare the different techniques used to determine indoor robot localization. Indoor Robot localization techniques are reviewed in Section II. In Section III, the NI robot platform functions and components are briefly reviewed. In Section IV, the localization experiments performed on the NI DANI robot to evaluate the accuracy of robot localization using the measured WiFi received signal strength (RSS), optical wheel encoder odometer, and ultrasonic sensor techniques are described including the LabVIEW program written to control the robot and capture the odometer and sensor readings. In Section V, the data results of the 3 explored localization methods are presented and the methods evaluated. The paper concludes in Section VI.

## 2. INDOOR MOBILE ROBOT LOCALIZATION TECHNIQUES

There are diverse methods to achieve indoor localization, depending on the environment, application, and availability. Localization technologies that use Radio frequency (RF) signals to estimate the target position have been popular lately amongst researchers. A brief description with potential for each wireless localization technology will be discussed in details.

*The Global Positioning System (GPS)* is one approach used for position indication. GPS depends on satellites orbiting the Earth and transmitting precise time radio signals. It provides a three dimensional position estimate in absolute coordinates by comparing the time delay from different satellite signals. Nowadays, the most accurate GPS's locates within an average of 2.5m CEP, which is not sufficient enough for accurate robot localization application. More importantly, the GPS signal tends to fade faster inside buildings [1] so it is more used in outdoor applications.

*GSM-based* indoor localization exploits GSM modules attaches to the moving target. The GSM module communicates with the closest base station around the area and calculates the probabilistic position of the target. Using GSM technology for localization has several features over other technologies. A localization system based on cellular signal has an advantage of utilizing the phone existing hardware without the need for additional radio interfaces. GSM coverage and capacity exceed the coverage and capacity of other technologies. Additionally, a cellular-based localization system is robust to indoor power failures [1].

*Infrared* is an energy radiation with a frequency below our eyes sensitivity. Based on the reflected signal, the infrared sensor could determine the location of the object. Multiple infrared transmitters and receivers are used for localization [1].

The purpose of the *Ultrasound (UT)* technique is to measure the distance between a fixed point and a mobile target using ultrasonic waves. The system must consist of one transmitter and multi receivers. In order to synchronize the receivers, a faster wave than ultrasonic is used such as radio or IR. After the receivers detect the reflected ultrasonic waves, they calculate the time between the synchronization signal and the reflected ultrasonic signal to estimate the distance between the transmitter and the target. The usefulness of this technique is the simplicity of implementation and the cost reduction. The main disadvantage of UT sensors is the generated multipath at

the receiver which could disturb the distance between the emitter and the target [1].

The *wireless local area network (WLAN)* technique requires information of either the travel time of the radio wave or the received signal strength in order to estimate the location. Using the IEEE 802.11 Wireless LAN for localization has fundamental benefits. First, the ubiquitous availability of WLAN access points in urban areas makes it easy to exploit for positioning purposes. Second, the WLAN approach results in bounded, not cumulative, positioning errors. Third, it outreaches the GPS signal in closed areas. Finally, flexibility of location and data ports is required. With the absence of line of sight, and the presence of path loss, multipath diversity and fading, the signal information becomes inaccurate and erroneous, which is considered as a drawback of WLAN [2].

There are some other physical technologies used for indoor localization purposes. *Odometer or encoder* is one of the oldest and basic techniques. It is usually attached to a wheel or motor cylinder to measure the actual rotation and estimate the distance traveled by the target [3]. *Camera localization* is being used for specific applications nowadays. The camera must deliver sufficient image quality in a decent lighting view for effective image processing. A reference object in each scene must be identified to estimate the instantaneous absolute position of the target away from it. High image processing and computational algorithms are required. Localization based on landmark recognition is yet another effective technique [3]. *Inertial measurement units (IMU)* technology is another concept that has been developed and improved for decades now. Each unit contains 3-axis accelerometer, 3-axis gyroscope, and other sensors. It uses the inertial property of a mass to calculate its motion. This concept is underdevelopment due to the unlimited cumulative errors of the sensors [4].

Every technology mentioned above has different advantages and limitations to the other technologies. Therefore, if we fuse two technologies that have complementary performance advantages, the localization accuracy will increase and the estimation errors will decline [4]. *Visual odometer* combines the data from an odometer and a camera to improve the localization accuracy of the target. This fusing algorithm is the one being applied currently on NASA's Mars Exploration Rover. The rover uses two pairs of stereo cameras in addition to wheels odometers [5].

New algorithms have been developed to assist localization technologies performance. L. Tian proposed an algorithm to estimate the position and orientation of an object based on RF signal strength [6]. H. Cheung utilized the mean and variance of the squared distance estimates to devise two linear least squares estimators for RSS-based localization [7].

Simultaneous Localization and Mapping (SLAM) is another technique to enhance the localization technologies [8].

The most effective localization technology will be the one that determines the target location by covering a wider area with acceptable range of error. The ubiquitous availability of WLAN indoor access points makes WLAN technology a good candidate to track targets in cost wise. Our experiments will test, compare the accuracy, and error range of WLAN localization with odometer and ultrasonic technologies.

### 3. DANI ROBOT DESCRIPTION AND DETAILS

The NI LabVIEW Robotics Starter Kit1, shown in Fig. 1, is a fully assembled mobile robot platform that features sensors, motors, NI single board reconfigurable I/O (sbRIO) hardware for embedded control. The simplicity of the DANI robot makes it ideal for prototyping mechatronic and robotic applications.

The sbRIO-963 embedded control and acquisition device integrates a real time processor, a user-reconfigurable-field-programmable gate array (FPGA), and I/O on a single board. The board can be programmed with LabVIEW Real-Time module, LabVIEW FPGA module, and LabVIEW Robotics Software. The sbRIO contains Serial and Ethernet ports for data communication.

Optical quadrature encoders are connected to the shaft between the motors and the wheels. They are incremental shaft encoders with 100 cycles per revolution, as shown in Fig. 2. Thus, it has a resolution of 400 pulses per revolution. Each encoder requires 5V power supplied by sbRIO.

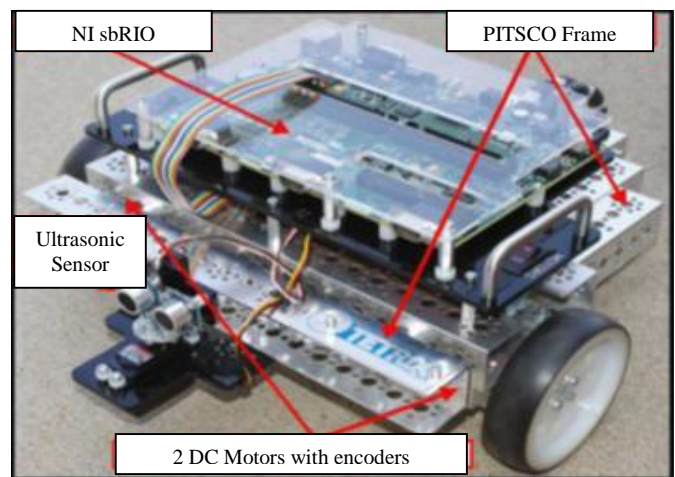


Figure 1: DANI Robot (Robotic Starter Kit1) [9]

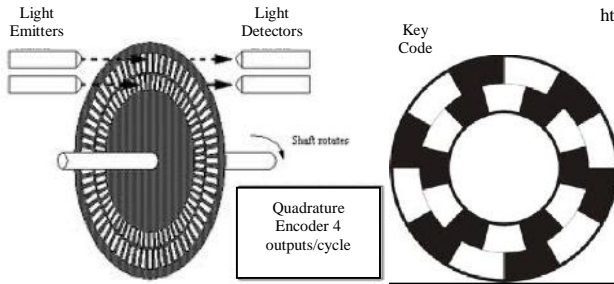


Figure 2: Quadrature Encoder [10], [11]

The Parallax PING)) 28015 ultrasonic sensor is attached to the DANI robot, and can detect objects by producing cyclic pressure wave with a frequency greater than 20 kHz (the upper limit of human hearing range). An ultrasonic pulse is transmitted from the probe under the trigger command. The pulse travels through the air around 340 m/s, hits an object, and bounces back to the sensor. Depending on the burst travel time, the sensor estimates the distance of the object away from the ultrasonic sensor. The transducer requires 5V supply power provided from the sbRIO and consumes around 20mA. The trigger command is sent from the BASIC stamp microcontroller integrated in the transducer to start the measurement. At the same time the PING piezoelectric transmitter will burst a short pulse converting electrical energy into sound with 40 kHz frequency. The piezoelectric receiver transducer will wait for the off-target reflected echo and refer it back to the microcontroller. The time difference between the transmission and reception of the pulse is the time the pulse takes to fly from the transducer to the target and come back. The distance between the transducer and the target is computed as

$$D = k \cdot T_f \cdot V_s \quad (1)$$

where

$T_f$  Time of flight of the ultrasonic pulse.

$V_s$  Velocity of sound in air.

$k$  A constant usually equal to 0.5 depends on the geometry of the transmitter and receiver transducers.

After the distance of the target is determined, the microcontroller will send it to the software through the sbRIO to process [12].

The PING)) is capable of measuring the distances of targets ranging from 0.02m to 3m. The transducer is mounted on the DANI robot on top of a 180 degrees sweeping servo motor, as shown in Fig. 3.



Figure 3: Parallax Ultrasonic Transducer

The wiring of the ultrasonic transducer, quadrature encoders, and sweeping servo motor are connected directly to digital input/output pins in the onboard sbRIO, while the DC motors are indirectly connected to the sbRIO pins through a driving circuit, which enables the motors to draw higher voltage and current that can only be provided by the battery not the controller. The DANI robot's battery delivers 12V and must be checked and charged before operation [13].

#### 4. EXPERIMENT AND CONTROL SOFTWARE PROGRAMMING

The purpose of our experiments is to determine the location of a robot moving along a line in an open area. The explored localization techniques are an odometer implemented by an optical wheel encoder mechanism, ultrasonic sensor and received WiFi WLAN signal strength. We will test, analyze and evaluate each technique.

The experiments were performed with a National Instrument (NI) robotic platform plus a WLAN communication system. The DANI robot was designed to be an explorer, in search and rescue, surveillance, retrieving, transporting, and other missions. It has a couple of DC motors to differentially drive the robot. The wheels connected to the motor are attached to odometer (quadrature encoder) to measure the actual wheel rotation and be used as a feedback for the controller. It comes with Parallax 28015 ultrasonic transducer mounted on top of a sweeping servo motor. However, the available ultrasonic sensor has limited range and accuracy. The motors and sensors of the robot are interfaced and controlled by a sbRIO\_9631, fixed on top of the DANI robot.

LabVIEW is the NI software for interfacing and programming the robot's controller, and interfacing and controlling the sensors and actuators through a DAC (Data Acquisition Card). The LabVIEW SDK was installed on a PXIe system and which the LabVIEW program to control the DANI robot was developed,

The NI PXIe-8133 is an embedded computer operated by windows and is capable of integrating various standard input/output modules. It has different communication ports, such as Ethernet to interface or program external controllers or

DAC's. This computer is the core of interfacing and programming the robot.

A wireless LAN (WLAN) router, situated in an adjacent hallway with a door separating it from the lab where the experiments were conducted, emitted a WiFi signal which was received by the mobile robot in the lab. We tried to connect a WLAN antenna to the DANI's sbRIO controller but we were missing receiver electronics. We instead opted to download the Net Stumbler application on a Samsung Galaxy SII mobile phone, running the Android operating system. We verified that the application works by moving the phone away from the router and then attached the Galaxy phone on top of the DANI robot [14].

The DANI robot was connected to the PXIe controller via Ethernet port in the sbRIO. After we had configured and tested the robot, the programming phase started on the PXIe. Our experiments were carried out on the DANI robot moving on a straight line on a clean floor and controlled by the NI PXI system running a LabVIEW program which starts and stops the robot, and reads wheel encoder and UT sensor data.

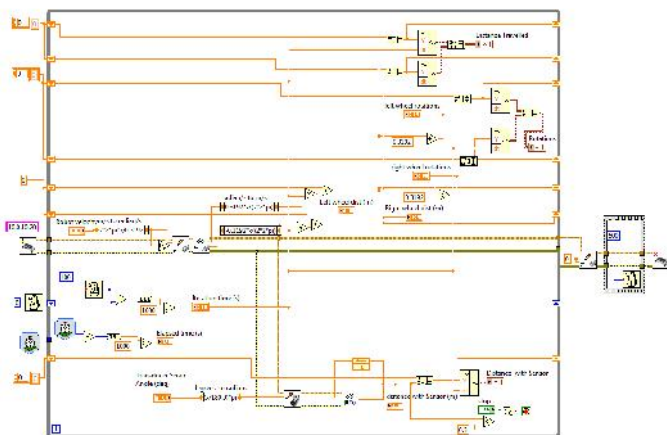


Figure 4: LabVIEW Block Diagram snapshot

The LabVIEW block diagram, shown in Fig. 4, is the main program that contains of objects, functions, structures, expressions, terminals, and wires to transfer data between other objects. The block diagram is developed on the PXIe embedded controller. Afterwards, the program was downloaded onto the sbRIO and processed in the FPGA on board of the mobile DANI robot. The first step in the software development after creating a project under the Starter Kit sbRIO tag was to establish a communication session with the FPGA on the DANI-Robot by placing the Initialize starter kit function in the Block Diagram Window. This step allowed the FPGA to access the different I/O's in the robot. The code that drives the robot and acquires the distance data was placed inside a while loop that terminates when a stop button is pressed by the operator. The motors' velocity is controlled by

the user before being sent to the DC motors velocity set point write function. The Read DC motor velocity Function returns the output of the two optical encoders. The velocities of the motors in every iteration are multiplied by the iteration time in order to get the distance traveled by each motor in every iteration. Shift registers are used to increment the total traveled distance by the current iteration traveled distance. Additionally, they are used to estimate the current iteration duration. In the same iteration, the read PING sensor distance block acquires the distance measurement output from the ultrasonic transducer. The output results of the optical encoder and the ultrasonic transducer are graphically displayed on the PXI screen. When the stop button is pressed, the while loop is terminated and the software closes the communication session with the DANI robot.

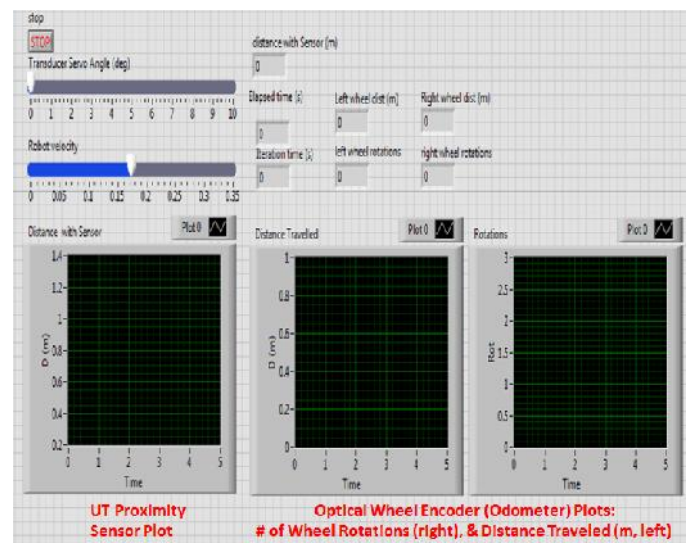


Figure 5: LabVIEW Front Panel snapshot

The GUI interface for the LabVIEW program, shown in Fig. 5, is called the Front Panel. It is mainly composed of the controls (inputs) and the indicators (outputs) of the program. The user controls the robot speed and transducer servo angle (shown on top left of the Figure). These inputs are relayed to the block diagram to be processed. The results of the block diagram are viewed in the front panel numerically or graphically. The program outputs the distance with UT sensor (top center) and the elapsed time, iteration time, left and right wheel rotations from the wheel encoders, and their converted distances (below top center). The interface also shows plots for the distances measured by the UT sensor and wheel encoders, respectively (bottom).

## 5. EXPERIMENT RESULTS AND RECOMMENDATIONS

We experimented with 3 localization methods: 1. Optical wheel encoder method; 2. Ultrasound sensor method; and 3. WIFI WLAN Received signal strength method. The line is

also marked by actual distance measurements using a measuring tape. The results of these experiments are presented in Table I and are plotted in Fig. 6. Periodically, the robot is stopped and the wheel encoder reading, UT sensor measurement, and WIFI received signal strength are all recorded at the travelled distance at which the robot is stopped.

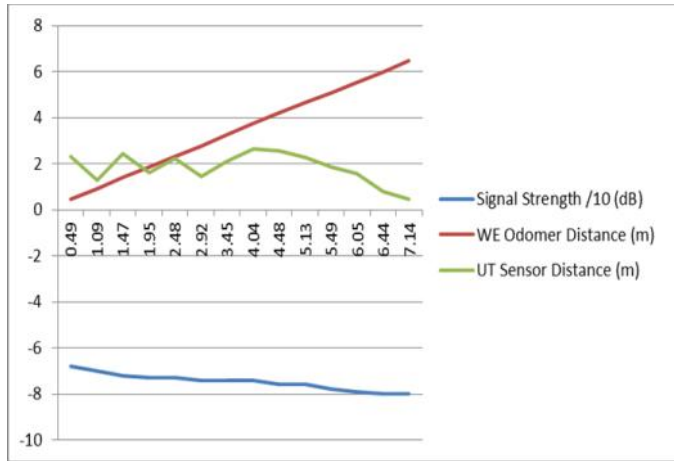


Figure 6: Three Localization Method Results Vs. Distance travelled by Robot

TABLE I. THE OBTAINED EXPERIMENTAL RESULTS

Distance (m)	Number of Rotations	Wheel Encoder Distance (m)	Sensor Distance (m)	Signal Strength (dB)
0.49	1.43	0.456699	2.32	-68
1.09	2.88	0.919786	1.27	-70
1.47	4.37	1.395647	2.45	-72
1.95	5.89	1.881089	1.62	-73
2.48	7.28	2.325014	2.22	-73
2.92	8.65	2.762551	1.43	-74
3.45	10.18	3.251187	2.12	-74
4.04	11.79	3.765372	2.63	-74
4.48	13.25	4.231653	2.56	-76
5.13	14.55	4.646834	2.29	-76
5.49	15.86	5.065208	1.88	-78
6.05	17.33	5.534682	1.57	-79
6.44	18.68	5.965832	0.79	-80
7.14	20.35	6.49918	0.45	-80

### A. Wheel Encoder Method

The distance traveled by the robot is the number of rotations times the wheel's circumference. The wheel's circumference is given by  $(2 * \pi * r)$ , where  $r$  is the wheel's radius.



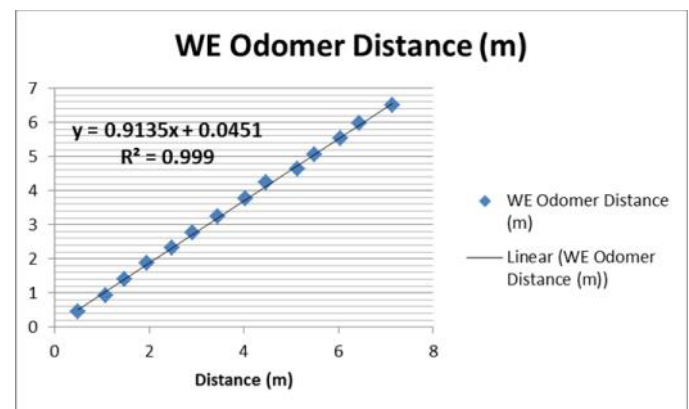
Figure 7: DANI Robot wheels

Fig. 7 shows the DANI robot wheels whose specifications are displayed in Table II.

TABLE II. Robot Wheel Specifications

Diameter:	10.166 cm
Circumference:	0.3192 m
Highest angular velocity:	15.7 rad/s
Small wheel gears teeth:	40
Large wheel gears teeth:	88

Fig. 6 plots the wheel encoder readings which correlate very well with the distance traveled by the robot. This is because the surface used is a smooth painted floor. The optical wheel encoder readings multiplied by the robot wheel's circumference give us the distance (in m) captured by the wheel encoder method. The 14 samples are plotted in Fig. 8 and the linear curve fit is displayed with very good correlation ( $R^2=0.999$ ). The  $R^2$  coefficient compares *actual*  $y$  coordinate and *estimated*  $y$  (on the fitted line), with  $R^2=1$  indicating perfect correlation, while  $R^2=0$  indicating poor linear fitting and unhelpful regression.

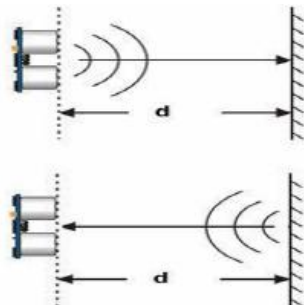


**Figure 8:** Wheel Encoder Distance Linear Interpolation

Prior work reveals that when the surface on which the wheels roll is slippery, the wheel encoder readings become compromised and lose their precision as the wheel may turn incrementing “the odometer” but in reality remains in its place. For this reason, other more reliable localization methods under slippery conditions are sought. The wheel encoder “odometer” method is thus a complimentary localization method which can be relied on under dry ideal surface conditions.

**B. Ultrasonic Sensor Method**

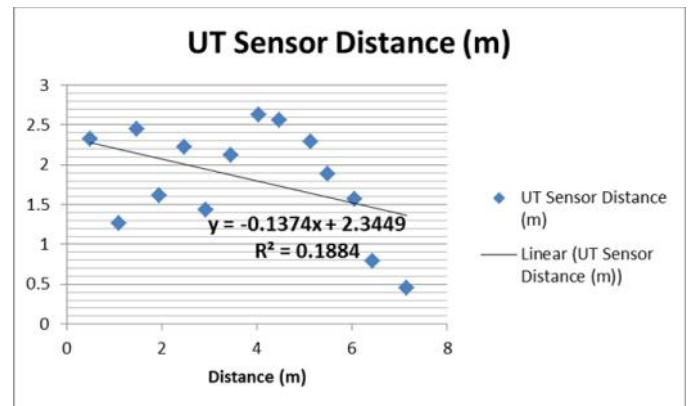
The UT sensor emits an UT signal, which bounces back after hitting a wall 8m away from robot’s start point, and is detected back by the sensor. The travel time of the reflected UT signal should correlate with the distance between the UT sensor and the reflecting surface. This process is illustrated in Fig. 9.



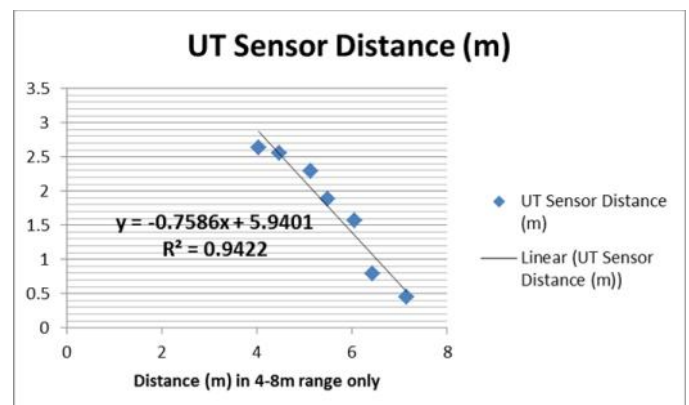
**Figure 9:** Ultrasonic Sensor Operation [5]

Fig. 6 plots the UT sensor readings at each robot stop. Between traveled distance of 0-4.04m (or about 4-8m away from the reflecting wall at the end of the robot line trajectory) the UT sensor readings are no reliable as they do not correlate with the traveled distance. The distances are in reference to the starting point, about 8m away from a reflecting wall at the end of the robot travel line. Smaller distances indicate closer proximity to the starting point and farness from the reflecting wall. In other words, a 0m distance means the robot is at the starting point, while an 8m distance means that the robot has reached the end near the reflecting wall. The linear interpolation of the UT sensor readings are plotted in Fig. 10 and indicate a poor linear fitting ( $R^2=0.1884$ ). After traveling for 4m, the robot is now closer to the reflecting wall at the end of the line, and is now within the UT sensor range of reliable operation. Thereafter, the UT sensor reading decreases with the distance traveled and the UT sensor more accurately measures the robot’s distance from the wall at the end of the line. When we only consider the UT sensor readings up to a distance of 8m-4m=4m away from the reflecting wall, the linear interpolation plot shown in Fig. 11 indicate improved correlation ( $R^2=0.9422$ ). The inaccurate measurements of the ultrasonic transducer in general are caused by ultrasonic signal

fading, specularity and beam width. As an acoustic wave propagates through a medium with a certain speed, a part of its energy is absorbed by the medium until it fades and is undetectable any more. Specularity considers the angle between the sound wave and the normal plane to the flat surface of the target. If this angle of reflection is too big, non-specular reflection will occur and no part of the wave will be reflected back to the transducer. Although the wide range of beam width enables the ultrasonic transducer to detect objects which are not directly in front of it, it decreases the accuracy of determining a pinpoint distance of an object. However, due to the physics of acoustic which limits the performance of ultrasonic sensors, a small beam width cannot achieved in reality. Moreover, there is a probability that the wave could reflect off of multiple surfaces before reaching the transducer causing false readings of the true distance ahead. Thus, using time of flight analysis only, of the ultrasonic transducer data, to determine the distance, results in inaccurate readings. Unlike other ranging techniques such as frequency modulation and Doppler Effect analysis that are far more complex than TOF and dramatically enhances the performance of the transducer. These analyses are used by bats sonar abilities [15-16].



**Figure 10:** Ultrasonic Sensor Distance Linear Interpolation



**Figure 11:** Ultrasonic Sensor Distance Linear Interpolation (within 4m of reflecting wall, only)

### C. Received WiFi Signal Strength Method

Our experiment consists of checking the signal strength with WLAN (by using Galaxy SII Android application) while the robot moves over the straight line.

Fig. 6 plots the received signal strength which correlates well with the distance traveled by the robot. When the robot travels for 6m from its start point (the router is now about 10 m away from the robot across the lab where the experiment was conducted in the hallway; a door separates the lab from the hallway), the accuracy of the received signal strength measurement slightly reduces as RSS measurements made at successive stops are identical or do not change much.

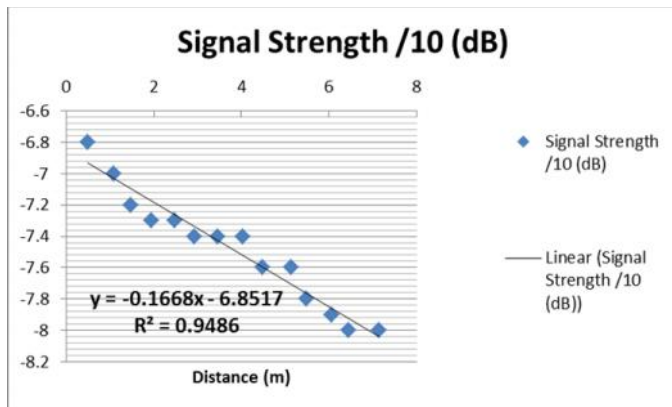


Figure 12: Received Signal Strength Linear Interpolation

The received WiFi signal strength readings (scaled by 1/10) are curve-fitted in Fig. 11 with very good correlation ( $R^2 = 0.9486$ ).

As expected the WiFi signal amplitude decreases with increasing the distance from the router's transmitting antenna. This phenomenon is called path loss which is considered the most important factor to characterize radio propagation model at the macroscopic level. The free space path loss expressions is shown in model (2)

$$\text{Free Space PL} = (4 \pi \cdot d \cdot f / c)^2 \quad (2)$$

where

- d** The propagation distance
- f<sub>c</sub>** Carrier frequency = 2.4 GHz
- c** Speed of light

Note that assuming there is always a line of sight between the transmitter and the receiver, the path loss effect in the free space increases proportionally with the square of the propagation distance and does not consider reflections or diffractions caused by obstacles nearby [17]. The inaccuracy of the measured signal strength could be caused by the effect of multipath fading where the same signal reaches the antenna through different paths at different times. This phenomenon

affects the result of the signal strength at a specific time and distance as the received signal strength may contain some portions of reflected, refracted old signals [18].

## 6. CONCLUSION

This paper explores and experiments with three localization techniques for indoor robots: optical wheel encoder "odometer-style" reading, Ultrasound sensor readings of UT signals bouncing back from a wall, and measured WiFi signal strength received from a WLAN router. Experiments are conducted on the NI DANI robot which is used as an explorer on a smooth surface area.

In ideal conditions with dry surface and non-slippery conditions, the optical wheel method is most accurate followed by the received signal strength method. In slippery or rough terrain conditions where the reliability of the optical wheel encoder method deteriorates and as long as the robot is under the operational range of the WiFi router and transmitter, the received WiFi signal strength method (possibly with extended antenna range) should be very accurate with a longer accuracy operational range than the UT sensor method.

In the near future, we plan to further explore the WiFi RSS method and transmitting router placements to extend its operational range.

## REFERENCES

- [1] O. Manu, "A Study of Indoor Localization Techniques", Stefan Cel Mare University.
- [2] P. Pivato, L. Fontana, L. Palopoli, and D. Petri, "Experimental Assessment of a RSS- based Localization Algorithm in Indoor Environment", *Proc. 2010 IEEE International Instrumentation and Measurement Technology Conference (I2MTC 2010)*, pp. 416-421, Austin, TX, U.S.A., 3-6 May 2010.
- [3] B. Siciliano, O. Khatib, *Handbook of Robotics*, Springer, 2008.
- [4] J. Seitz, L. Patino, B. Schindler, S. Haimerl, "Sensor Data Fusion for Pedestrian Navigation Using WLAN and INS," *Symposium Gyro Technology 2007*, Karlsruhe, Germany, 2007.
- [5] Y. Cheng, M. Maimone, and L. Matthies, "Visual Odometry on the Mars Exploration Rovers," *Proc. IEEE Conf. on Systems, Man and Cybernetics*, The Big Island.
- [6] T. Longqiang, et al., "A Novel 5-Dimensional Indoor Localization Algorithm Based on RF Signal Strength," *Proceedings of the IEEE International Conference on Automation and Logistics Shenyang, China, August 2009*.
- [7] Hing Cheung So and Lanxin Lin, "Linear Least Squares Approach for Accurate Received Signal Strength Based Source Localization," *IEEE Transactions on Signal Processing*, Vol. 59, No. 8, August 2011.
- [8] H. Durrant-Whyte, T. Bailey, "Simultaneous Localization and Mapping: Part I", *IEEE Robotics & Automation Magazine*, June 2006.
- [9] R. King, "Mobile Robotics Experiments with DANI," [download.ni.com/pub/devzone/.../mobile\\_robotics\\_experiments.pdf](http://download.ni.com/pub/devzone/.../mobile_robotics_experiments.pdf)
- [10] <http://www.romanblack.com>
- [11] <http://www.barrgroup.com>

<http://www.cisjournal.org>

- [12] A. Carullo, M. Parvis, "An Ultrasonic Sensor for Distance Measurement in Automotive Applications", IEEE Sensours Journal, VOL. 1, NO. 2, Aug 2001.
- [13] National Instrument , <http://www.ni.com>.
- [14] Netstumbler on Android System, <http://www.stumbler.net> ; or  
[http://www.androidzoom.com/android\\_applications/netstumbler](http://www.androidzoom.com/android_applications/netstumbler)
- [15] Farhaz Karmali, Andrew Tomlinson, Harshit Goyal, "Characterization of a Parallax PING)) Ultrasonic Range Finder", www.eng.auburn.edu.
- [16] William R. Hendee and E. Russell Ritenour, "Medical Imaging Physics", Fourth Edition.
- [17] Fabiana Capulli, et al., "Path Loss Models for IEEE 802.11a WLAN", IEEE Wireless Communication Systems, 2006.
- [18] Ma DongLin, Lai Fansheng, Sun Jie, "Simulation on multi-path fading in wireless channel", IEEE (ICCSEE), 2012.



**Pablo Carrasco** is currently with Saudi Aramco, R&DC in Saudi Arabia. He received the M.S. in Mechanical Engineering in 2011 from King Abdullah University of Science & Technology, KSA, and the B.S. in Mechatronics Engineering in 2009 from Monterrey Institute of Technology and Higher Studies (ITESM), Mexico. He previously worked for 2 years

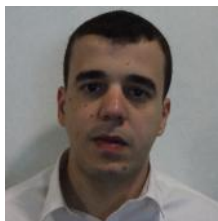
as an intern for Procter & Gamble, Control & Information Systems unit of the Household Care Business Line in robotics, automation and control for cost savings projects. His main fields of interest are mechatronics, robotics, control, intelligent systems and mechanical design.

## AUTHOR PROFILES



**Fadi Sibai** is with the R&D Center, Saudi Aramco, Saudi Arabia and has over 24 years of post doctoral experience. He received the Ph.D. degree in Electrical Engineering from Texas A&M University. He previously worked for Intel Corporation, USA, and held academic positions in the US and the Middle East. He authored or coauthored more than 150 technical

publications and reports, and served on the organizing or program committees of more than 20 international conferences. His strengths are in embedded systems, networks, high-performance computing, and intelligent systems. His biography is published in the 2011 editions of Who's Who in the World and IBC's 2000 Outstanding Intellectuals of the 21st Century. He is a member of Eta Kappa Nu, the Society of Petroleum Engineers, and is a senior member of the Institute for Electrical and Electronic Engineers (IEEE).



**Hassane Trigui** is currently with Saudi Aramco, R&DC in Saudi Arabia. He received the M.S. in Communications and Signal Processing in 2011 from King Abdullah University of Science & Technology, KSA, and the Bachelor in Control and Instrumentation Systems Engineering in 2009 from King Fahd University for Petroleum & Minerals, KSA. His main fields of interest are

wireless communication, intelligent systems, control, robotics and instrumentation.